

MEG Spatio-Temporal Analysis Using a Covariance Matrix Calculated from Nonaveraged Multiple-Epoch Data

Kensuke Sekihara,* *Member, IEEE*, David Poeppel, Alec Marantz, Hideaki Koizumi, and Yasushi Miyashita

Abstract— We propose a magnetoencephalographic (MEG) spatio-temporal analysis in which the measurement-covariance matrix is calculated using nonaveraged multiple epoch data. The proposed analysis has two advantages. First, a very narrow time window can be used for the source estimation. Second, accurate localization is possible even when the source activation has a time jitter. Experiments using auditory evoked MEG data clearly demonstrate these advantages.

Index Terms—Biomagnetics, biomedical electromagnetic imaging, biomedical signal processing, functional brain imaging, inverse problems.

I. INTRODUCTION

SPATIO-TEMPORAL modeling [1], [2] is known to reduce the degree of the ill-posedness in the biomagnetic inverse problem [3]. In this modeling, a measurement-covariance matrix (or equivalently a spatio-temporal data matrix) is constructed, and source locations are estimated using this covariance matrix, assuming that the source locations are unchanged during the measurement.

It is common in studies of evoked neuromagnetic fields to measure many epochs by applying a stimulus repeatedly and to analyze the data averaged over these epochs. When applying the spatio-temporal analysis to such evoked field data, the measurement-covariance matrix is calculated by using this averaged data. This conventional way of calculating the measurement-covariance matrix has two problems.

First, the time window for calculating the covariance matrix must be large enough to contain a sufficient number of time points to ensure the accuracy of the sample covariance matrix. The use of a large window, however, may result in

an erroneous source localization, if the source configuration rapidly changes within this time window. Second, averaging the multiple-epoch data obviously assumes that all the epochs are time-locked to the stimulus. Thus, when a nontime-locked source exists, the source estimation may also be erroneous.

In this paper, we propose to calculate the measurement-covariance matrix directly from nonaveraged multiple-epoch data. By calculating the measurement-covariance matrix from nonaveraged data, the source localization can be carried out using a small time window, which is advantageous when the source configuration changes rapidly. Also, source localization using this covariance matrix is not influenced by whether the source activation is time-locked or not, and the location of a source whose activation onset has a time jitter in each epoch can be accurately estimated.

One difficulty with the use of nonaveraged data is that the data inevitably contains a large amount of background spontaneous activity that is usually averaged out. In this paper, this difficulty is circumvented by the use of a prewhitening technique that incorporates the noise covariance matrix obtained using the prestimulus parts of the nonaveraged data. Specifically, we use the previously proposed prewhitening MUSIC algorithm [4], [5], as the source localization procedure. The MUSIC algorithm has the distinct advantage of providing a suboptimal solution by using only a three-dimensional search, regardless of the number of sources. The use of the MUSIC algorithm, however, is not essential to implement the proposed method. Any other source estimation method [6] can be used together with the prewhitening technique.

Section II describes our proposed analysis, followed by a brief explanation of the prewhitening MUSIC algorithm. Section III presents the results of our experiments which show the effectiveness of the proposed analysis. Throughout this paper, plain italics indicate scalars, lower-case boldface italics indicate vectors, and upper-case boldface italics indicate matrices. The superscript T indicates the matrix transpose. The eigenvalues are numbered in decreasing order.

II. METHOD

A. Prewhitening MUSIC Algorithm

The prewhitening MUSIC algorithm was proposed to reduce the influence of the background activity by taking its

Manuscript received August 7, 1997; revised November 19, 1998. This work was supported in part by the MIT-JST International Research Project "Mind Articulation." Asterisk indicates corresponding author.

*K. Sekihara is with the Mind Articulation Project, Japan Science and Technology Corporation (JST), Yushima 4-9-2, Bunkyo-ku, Tokyo 113-0034, Japan (e-mail: sekihara@ma.jst.go.jp).

D. Poeppel is with the Department of Linguistics and Biology, University of Maryland, College Park, MD 20742 USA.

A. Marantz is with the Department of Linguistics and Philosophy, Massachusetts Institute of Technology, Cambridge, MA 02139 USA.

H. Koizumi is with the Mind Articulation Project, Japan Science and Technology Corporation (JST), Tokyo 113-0034, Japan.

Y. Miyashita is with the Mind Articulation Project, Japan Science and Technology Corporation (JST), Tokyo 113-0034, Japan. He is also with the Department of Physiology, The University of Tokyo, School of Medicine, Hongo, Tokyo 113-0033, Japan.

Publisher Item Identifier S 0018-9294(99)03114-6.

covariance matrix into account [5]. It can provide accurate source estimation results even when a large amount of background activity exists. Since the details of the prewhitening MUSIC algorithm have already been reported [5], it is only briefly explained here for the reader's convenience. We define the magnetic-field data measured by the m th detector coil at time t as $b_m(t)$, and also define a vector $\mathbf{b}(t) = (b_1(t), b_2(t), \dots, b_M(t))^T$ as a set of measured data where M is the total number of detector coils. The spherical homogeneous conductor [7] is assumed, so we consider two tangential components, the ϕ and θ components, of the source moment and assume the radial component is zero. For simplicity, we assume that all sources have fixed orientations during measurement. The lead field vectors for the ϕ and θ components of the source at \mathbf{x} are defined as $\mathbf{l}_\phi(\mathbf{x}) = (l_1^\phi(\mathbf{x}), l_2^\phi(\mathbf{x}), \dots, l_M^\phi(\mathbf{x}))^T$ and $\mathbf{l}_\theta(\mathbf{x}) = (l_1^\theta(\mathbf{x}), l_2^\theta(\mathbf{x}), \dots, l_M^\theta(\mathbf{x}))^T$. We define the lead field matrix for the source at \mathbf{x} as $\mathbf{L}(\mathbf{x}) = [\mathbf{l}_\phi(\mathbf{x}), \mathbf{l}_\theta(\mathbf{x})]$.

Let us denote the measurement-covariance matrix as \mathbf{R}_b , and the noise covariance matrix as \mathbf{R}_n . Let us define $\tilde{\mathbf{e}}_j$ as an eigenvector obtained by solving the generalized eigenvalue problem, $\mathbf{R}_b \tilde{\mathbf{e}}_j = \lambda_j \mathbf{R}_n \tilde{\mathbf{e}}_j$, and $\tilde{\mathbf{E}}_N$ as $\tilde{\mathbf{E}}_N = [\tilde{\mathbf{e}}_{P+1}, \dots, \tilde{\mathbf{e}}_M]$ where P is the number of sources. The prewhitening MUSIC algorithm makes use of the fact that the noise subspace projector $\tilde{\mathbf{E}}_N \tilde{\mathbf{E}}_N^T$ and $\boldsymbol{\eta}_{opt}^T \mathbf{L}^T(\mathbf{x})$ are orthogonal at the true source locations, where $\boldsymbol{\eta}_{opt}^T = (\eta_\phi, \eta_\theta)$ represents the normal vector of the source orientation that gives the maximum orthogonality. This orthogonality can be checked by calculating the following localization function:

$$J(\mathbf{x}) = 1/\lambda_{\min}(\mathbf{L}(\mathbf{x})^T \tilde{\mathbf{E}}_N \tilde{\mathbf{E}}_N^T \mathbf{L}(\mathbf{x}), \mathbf{L}^T(\mathbf{x}) \mathbf{R}_n^{-1} \mathbf{L}(\mathbf{x})) \quad (1)$$

where $\lambda_{\min}(\cdot, \cdot)$ indicates the minimum generalized eigenvalue of the matrix pair in the parenthesis. The prewhitening MUSIC algorithm detects the source locations by calculating this localizing function in a volume where sources can exist, and by choosing each location where this localizing function reaches a peak as one dipole source location. It is worth noting that the localizing function for nonprewhitening MUSIC is [8]

$$J(\mathbf{x}) = 1/\lambda_{\min}(\mathbf{L}(\mathbf{x})^T \mathbf{E}_N \mathbf{E}_N^T \mathbf{L}(\mathbf{x}), \mathbf{L}^T(\mathbf{x}) \mathbf{L}(\mathbf{x})) \quad (2)$$

where $\mathbf{E}_N = [e_{P'+1}, \dots, e_M]$, and \mathbf{e}_j is an eigenvector obtained by solving the ordinary eigenvalue problem, $\mathbf{R}_b \mathbf{e}_j = \lambda_j \mathbf{e}_j$. Here, P' is the number of sources; P' may be different from P because in nonprewhitening cases, sources for the background activity may need to be taken into account.

B. Proposed Spatio-Temporal Analysis Using Nonaveraged Data

1) *Conventional Covariance Matrix Calculation:* Because calculating the covariance matrix theoretically requires an infinite number of measurements, some kind of approximation needs to be introduced in practice. In this subsection, we describe both the conventional and proposed methods of calculating the measurement-covariance matrix, explaining the difference between them.

Let us decompose the nonaveraged measured magnetic field $\mathbf{b}(t)$ into the four components: $\mathbf{b}^L(t)$, $\mathbf{b}^U(t)$, $\mathbf{b}^D(t)$, and $\mathbf{n}(t)$,

$$\mathbf{b}(t) = \mathbf{b}^L(t) + \mathbf{b}^U(t) + \mathbf{b}^D(t) + \mathbf{n}(t). \quad (3)$$

Here, $\mathbf{b}^L(t)$ is the signal evoked-magnetic field that is time-locked to the stimulus, $\mathbf{b}^U(t)$ is the signal evoked-magnetic field that is not time-locked to the stimulus and has a time jitter in each activation onset, $\mathbf{b}^D(t)$ is the background field disturbance caused by external sources such as magnetocardiography (MCG) interference or spontaneous neuromagnetic activity, and $\mathbf{n}(t)$ is the intrinsic sensor noise approximated by the white Gaussian noise with variance σ^2 .

We assume that a total of K_e epochs are measured. We denote the summation over these K_e epochs as \sum_{epoch} . Then, the averaged field $\tilde{\mathbf{b}}(t)$, $\tilde{\mathbf{b}}^L(t)$, $\tilde{\mathbf{b}}^U(t)$, $\tilde{\mathbf{b}}^D(t)$, and $\tilde{\mathbf{n}}(t)$ are defined as: $\tilde{\mathbf{b}}(t) = (1/K_e) \sum_{\text{epoch}} \mathbf{b}(t)$, $\tilde{\mathbf{b}}^L(t) = (1/K_e) \sum_{\text{epoch}} \mathbf{b}^L(t)$, $\tilde{\mathbf{b}}^U(t) = (1/K_e) \sum_{\text{epoch}} \mathbf{b}^U(t)$, $\tilde{\mathbf{b}}^D(t) = (1/K_e) \sum_{\text{epoch}} \mathbf{b}^D(t)$, and $\tilde{\mathbf{n}}(t) = (1/K_e) \sum_{\text{epoch}} \mathbf{n}(t)$. Here, we can assume that $\tilde{\mathbf{b}}^L = \mathbf{b}^L(t)$ and $\tilde{\mathbf{b}}^D(t) \approx 0$. Accordingly, we have

$$\tilde{\mathbf{b}}(t) \approx \mathbf{b}^L(t) + \tilde{\mathbf{b}}^U(t) + \tilde{\mathbf{n}}(t). \quad (4)$$

The conventional way of obtaining the measurement-covariance matrix is to calculate the time average during a certain time period. Let us denote the measurement-covariance matrix obtained in this manner as $\tilde{\mathbf{R}}_b$. The summation over time is denoted as \sum_t and the number of time points used in this summation is denoted as K_t . Then, we have

$$\tilde{\mathbf{R}}_b = \frac{1}{K_t} \sum_t \tilde{\mathbf{b}}(t) \tilde{\mathbf{b}}^T(t) \approx \tilde{\mathbf{R}}_b^{ev} + \frac{\sigma^2}{K_e} \mathbf{I} \quad (5)$$

where \mathbf{I} is the unit matrix and $\tilde{\mathbf{R}}_b^{ev}$ is obtained from

$$\tilde{\mathbf{R}}_b^{ev} = \frac{1}{K_t} \sum_t (\mathbf{b}^L(t) + \tilde{\mathbf{b}}^U(t)) (\mathbf{b}^L(t) + \tilde{\mathbf{b}}^U(t))^T. \quad (6)$$

In deriving (5), we assume that $(1/K_t) \sum_t \tilde{\mathbf{n}}(t) \tilde{\mathbf{n}}^T(t) = (\sigma^2/K_e) \mathbf{I}$. If the nontime-locked evoked activity $\mathbf{b}^U(t)$ does not exist, the measurement-covariance matrix $\tilde{\mathbf{R}}_b$ is reduced to

$$\tilde{\mathbf{R}}_b = \mathbf{R}_b^L + \frac{\sigma^2}{K_e} \mathbf{I} \quad (7)$$

where $\mathbf{R}_b^L = (1/K_t) \sum_t \mathbf{b}^L(t) (\mathbf{b}^L(t))^T$. Thus, in this case, $\tilde{\mathbf{R}}_b$ can provide accurate information regarding the evoked activity $\mathbf{b}^L(t)$ and accurate localizations of the sources for $\mathbf{b}^L(t)$ can be obtained using this $\tilde{\mathbf{R}}_b$.

However, two problems arise when utilizing (5). First, to obtain sufficient accuracy, a fairly large number of time points are needed to calculate the sample covariance matrix. Second, when the time-unlocked activity $\mathbf{b}^U(t)$ cannot be ignored, the source estimation obtained from $\tilde{\mathbf{R}}_b$ may contain errors caused by the activity $\mathbf{b}^U(t)$.

2) *Proposed Covariance Matrix Calculation*: In this paper, instead of using (5), we propose to calculate the measurement-covariance matrix using nonaveraged field data, such that

$$\hat{\mathbf{R}}_b = \frac{1}{K_e K_t} \sum_{\text{epoch}} \sum_t \mathbf{b}(t) \mathbf{b}^T(t) = \hat{\mathbf{R}}_b^{ev} + \hat{\mathbf{R}}_b^D + \sigma^2 \mathbf{I} \quad (8)$$

where $\hat{\mathbf{R}}_b^{ev}$ and $\hat{\mathbf{R}}_b^D$ are the covariance matrices for evoked activities and for the background disturbance. These matrices are obtained from

$$\hat{\mathbf{R}}_b^{ev} = \frac{1}{K_e K_t} \sum_{\text{epoch}} \sum_t (\mathbf{b}^L(t) + \mathbf{b}^U(t)) (\mathbf{b}^L(t) + \mathbf{b}^U(t))^T \quad (9)$$

and

$$\hat{\mathbf{R}}_b^D = \frac{1}{K_e} \cdot \frac{1}{K_t} \sum_{\text{epoch}} \sum_t \mathbf{b}^D(t) (\mathbf{b}^D(t))^T. \quad (10)$$

In deriving (8), we assume that the evoked activities are uncorrelated with the background activity. Equation (8) shows that the covariance matrix $\hat{\mathbf{R}}_b$ contains information regarding the signal source to be measured $\hat{\mathbf{R}}_b^{ev}$ as well as regarding the influence of the disturbance $\hat{\mathbf{R}}_b^D$. However, if we obtain the noise covariance matrix $\hat{\mathbf{R}}_n$, which is equal to $\hat{\mathbf{R}}_b^D + \sigma^2 \mathbf{I}$, we can reduce the influence of the background disturbance by applying a prewhitening technique. We show in the following section that the previously proposed prewhitening MUSIC algorithm [5] can almost completely remove this influence.

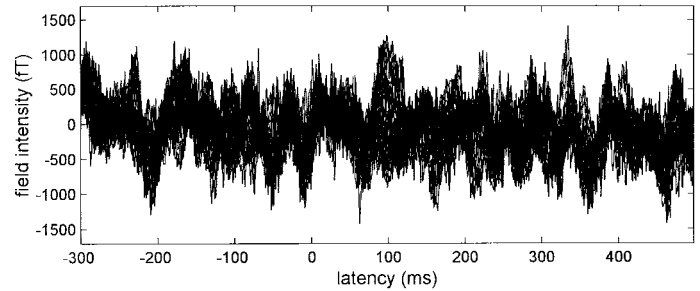
III. EXPERIMENTS USING AUDITORY-EVOKED FIELD DATA

A. General Description

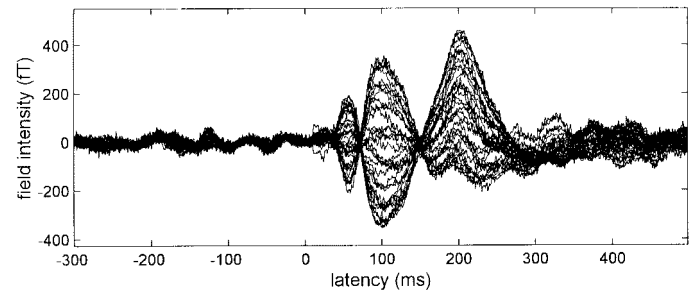
We performed source localization experiments using actual auditory-evoked data to test the effectiveness of the proposed analysis. The auditory-evoked fields elicited by a 1000-Hz pure tone of 400-ms duration were measured using a 37-channel Magnes magnetometer installed at the Biomagnetic Imaging Laboratory, University of California, San Francisco. All measurements were done in a magnetically shielded room. The stimulus was presented to the subject's right ear, and the sensor array was placed above the subject's left hemisphere with the position adjusted to optimally record the N1m auditory evoked field.

Two-hundred-fifty-six epochs were measured with the average interstimulus interval of 2 s randomly varied between 1.75 and 2.25 s. The sampling frequency was set at 1 kHz, and the data was collected from -300 ms before the stimulus onset to 700 ms after it. An on-line filter with the bandwidth from 1–400 Hz was used, and no additional digital filter was applied. One of the 256 epochs and the field data averaged over all the epochs are shown in Fig. 1(a) and (b), respectively. In Fig. 1(a), the single-epoch data contains a large amount of spontaneous activity, but in (b), much of this activity was suppressed through the averaging.

The x , y , and z coordinates used to express the estimated results are depicted in Fig. 2. These coordinates are measured in centimeters. The measurement-covariance matrix $\hat{\mathbf{R}}_b$ was



(a)



(b)

Fig. 1. Auditory evoked response used in the experiments: (a) one of the 256 raw epoch data and (b) the data averaged over 256 epochs. The data portion from -300 to 500 ms is shown.

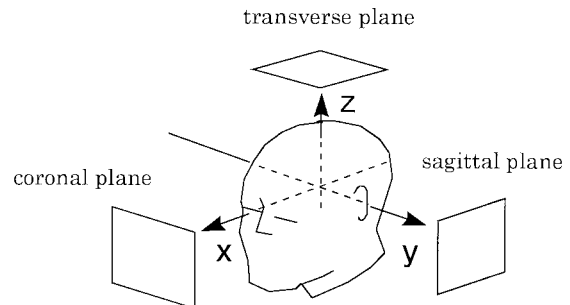


Fig. 2. The x , y , and z coordinates used to express the estimated results. The midpoint between the left and right preauricular points is defined as the coordinate origin. The axis directed away from the origin toward the left preauricular point is defined as the $+y$ axis, and that from the origin to the nasion is the $+x$ axis. The $+z$ axis is defined as the axis that is perpendicular to both these axes and directed from the origin to the vertex.

calculated, by using (5). The averaged field data shown in Fig. 1(b) was used with the time window between 0 and 100 ms. The results of applying the nonprewhitening MUSIC algorithm with this covariance matrix is shown in Fig. 3. The MUSIC localizing function in (2) was calculated with an interval of 0.5 cm over a volume defined as $-4 \leq x \leq 6$, $0 \leq y \leq 7$, and $3 \leq z \leq 11$. The figure shows that the algorithm detected the N1m source, which is believed to be located in the primary auditory cortex area.

B. Detecting a Source Using a Small Time Window

We calculated the measurement-covariance matrix $\hat{\mathbf{R}}_b$ with the time window between 98 and 102 ms. This time window was selected because it includes the N1m peak. Only six time

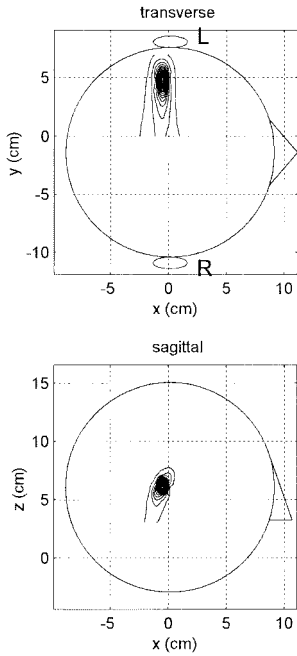


Fig. 3. The results of plotting the nonprewhitening MUSIC localizer from (2) when applied to the averaged data shown in Fig. 1(b) with the time window between 0 and 100 ms. The localizer was calculated with an interval of 0.5 cm within a volume defined as $-4 \leq x \leq 6$, $0 \leq y \leq 7$, and $3 \leq z \leq 11$; the projections of the localizer values onto the transverse, coronal, and sagittal planes are shown. The circles depicting a human head represent the projections of the sphere used to calculate the forward solution. *L* and *R* indicate the subject's left and right hemispheres.

points were used to calculate $\tilde{\mathbf{R}}_b$. The results of plotting the nonprewhitening MUSIC localization function (2) are shown in Fig. 4. In these results, the distortion is so severe that no source can be detected due to the inaccuracy of the sample covariance matrix.

We then calculated the covariance matrix $\hat{\mathbf{R}}_b$ using (8) with the same time window between 98 and 102 ms. The noise covariance matrix $\hat{\mathbf{R}}_n$ was calculated with the time window between -300 and 0 ms. The nonprewhitening MUSIC algorithm was first applied using only $\hat{\mathbf{R}}_b$. The results are shown in Fig. 5. In these results, the N1m source and another source were detected; the second source was probably caused by the spontaneous activity. The prewhitening MUSIC algorithm was then applied using both $\hat{\mathbf{R}}_b$ and $\hat{\mathbf{R}}_n$, and the results are shown in Fig. 6. In these results, only the single source located in the primary auditory cortex area is clearly detected.

A comparison between Figs. 4 and 6 demonstrates the effectiveness of calculating the measurement-covariance matrix with the nonaveraged multiple-epoch data when the time window is very small. The comparison between Figs. 5 and 6 shows the necessity of applying a prewhitening technique when dealing with nonaveraged data.

Note that in theory the proposed covariance matrix is subject to a stronger influence from the uncorrelated sensor noise than the conventional covariance matrix is. This can be understood by noting that the sensor-noise influence is represented by $(\sigma^2/K_e)\mathbf{I}$ in (5), whereas its influence is represented by $\sigma^2\mathbf{I}$ in (8). However, when comparing Figs. 3 and 6, the

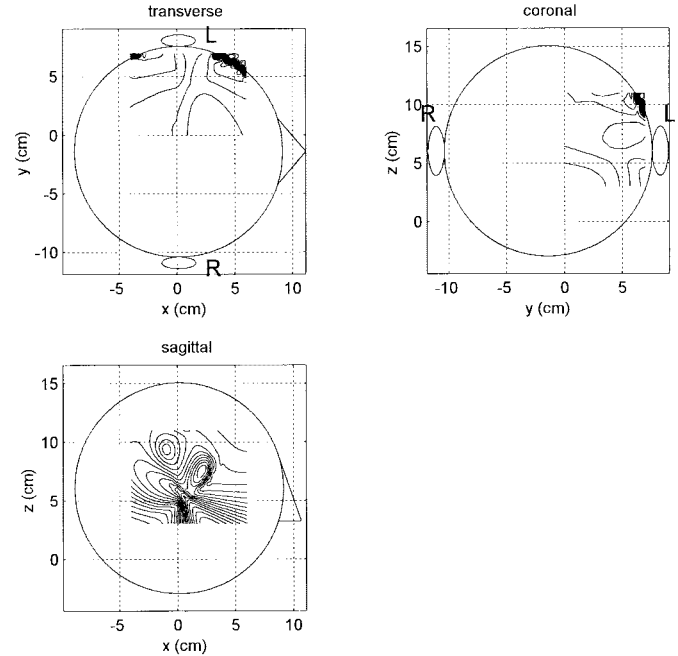


Fig. 4. The results of applying the nonprewhitening MUSIC algorithm to the averaged data with a small time window between 98 and 102 ms.

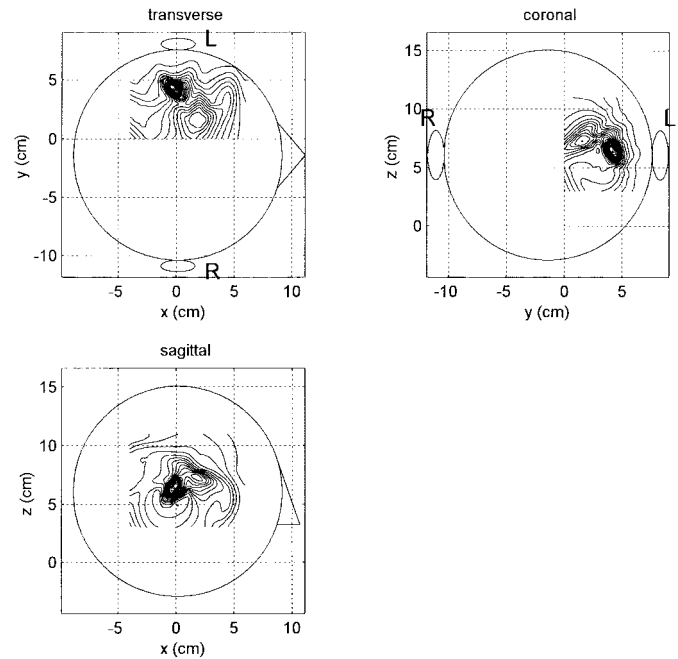


Fig. 5. The results of applying the nonprewhitening MUSIC algorithm to nonaveraged data. The covariance matrix $\hat{\mathbf{R}}_b$ was calculated by using (8) with the time window between 98 and 102 ms.

greater influence of the sensor noise is not evident. This is probably because the sensor noise in most modern biomagnetic instruments, such as the one used in the current experiment, is too low to influence the final source localization results, even when nonaveraged data is used.

To further investigate this point, we check the eigenvalue spectra of the covariance matrices $\tilde{\mathbf{R}}_b$ and $\hat{\mathbf{R}}_b$. The spectrum

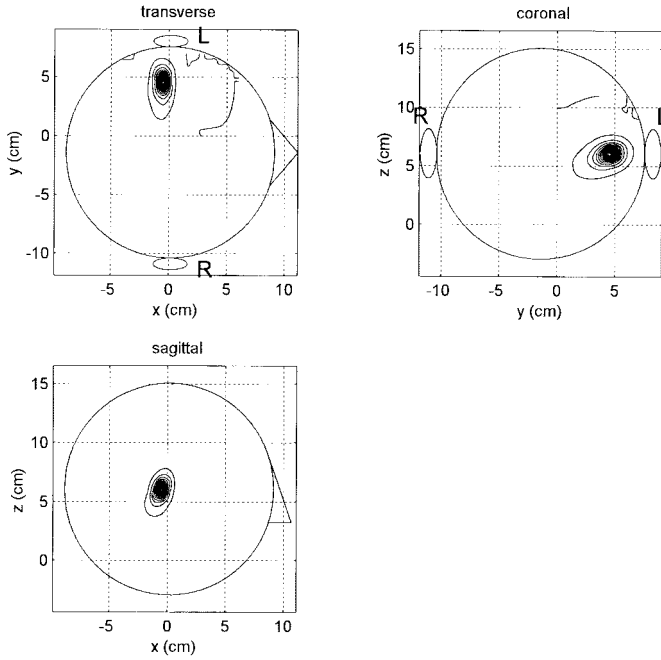


Fig. 6. The results of applying the prewhitening MUSIC algorithm to nonaveraged data with the time window between 98 and 102 ms. The same covariance matrix $\hat{\mathbf{R}}_b$ as used to obtain the results in Fig. 5 was used. The noise covariance matrix $\hat{\mathbf{R}}_n$ was calculated with the time window between -300 and 0 ms.

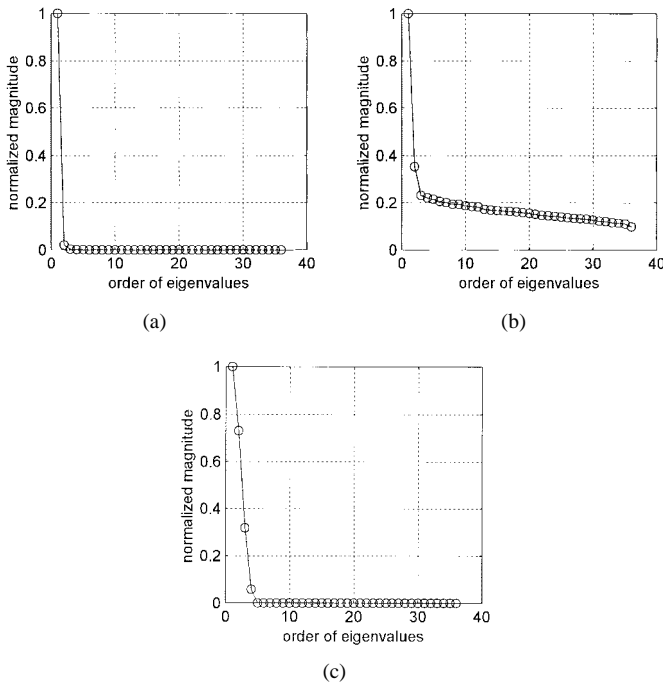


Fig. 7. (a) Eigenvalue spectrum of $\hat{\mathbf{R}}_b$ used to obtain the results shown in Fig. 3, (b) that of $\hat{\mathbf{R}}_b$ used to obtain the results shown in Fig. 6, and (c) that of $\hat{\mathbf{R}}_b$ used to obtain the results shown in Fig. 4.

in Fig. 7(a) relates to the results found in Fig. 3, the spectrum in Fig. 7(b) relates to the results in Fig. 6, and the spectrum in Fig. 7(c) relates to the results in Fig. 4. In Fig. 7(a), the first eigenvalue is distinctively large and the second one is larger than the other noise-level eigenvalues. Thus, we set

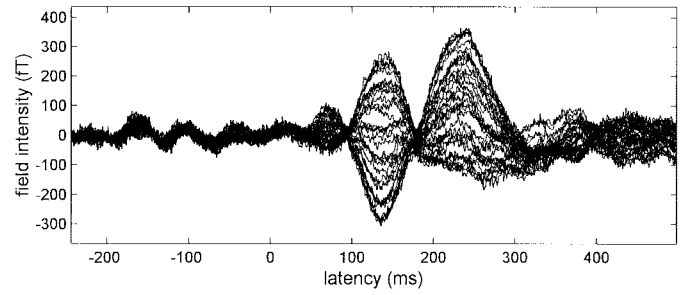


Fig. 8. The magnetic field averaged over 256 raw epoch data with an artificial time-jitter. The jitter was created with a uniform random number distributed between 0 and 60 ms.

$P = 2$ in order to obtain the results shown in Fig. 3. In Fig. 7(b), the noise-level eigenvalues are much larger than those in Fig. 7(a) because $\hat{\mathbf{R}}_b$, which was used to obtain the results in Fig. 6, contained the influence of the large sensor noise from raw-epoch data. Nonetheless, we can still observe two eigenvalues that are clearly larger than the noise-level eigenvalues in this spectrum. Therefore, we were able to separate the signal subspace from the noise subspace even though a strong influence of the large sensor noise was contained in the covariance matrix. In Fig. 7(c), however, false signal-level eigenvalues arose due to the inaccuracy in the sample covariance matrix, and as a result, the noise subspace was inaccurately estimated.

C. Detecting a Source Whose Activation Onset Has a Time Jitter

We next tested the effectiveness of the proposed analysis in detecting a source whose activation onset varies from epoch to epoch. To generate the data used for this experiment, we artificially created a jitter for each epoch data. That is, each epoch measurement $\mathbf{b}(t)$ was artificially time shifted to create $\mathbf{b}(t+t_z)$. Here, t_z was a uniform random number generated in a computer and it was distributed between 0 and 60 ms. The field data averaged over all epochs were calculated using

$$\tilde{\mathbf{b}}(t) = \frac{1}{256} \sum_{\text{epoch}} \mathbf{b}(t+t_z). \quad (11)$$

This averaged magnetic field $\tilde{\mathbf{b}}(t)$ is shown in Fig. 8. Comparing this figure with Fig. 1(b), we can see that the peak at approximately 50 ms of latency became less clearly defined due to the artificially introduced time jitter t_z . In addition, the appearance of the N1m peak was modified.

The covariance matrix $\hat{\mathbf{R}}_b$ was calculated using this averaged field data with a time window between 30 and 130 ms. The results of the nonprewhitening MUSIC algorithm obtained using this $\hat{\mathbf{R}}_b$ are shown in Fig. 9. These results contain severe blurring and no accurate source estimation can be made. We then calculated the covariance matrix $\hat{\mathbf{R}}_b$ by using (8) with the same time window between 30 and 130 ms. The noise covariance matrix $\hat{\mathbf{R}}_n$ was calculated with the time window between -240 and 0 ms. First, the nonprewhitening MUSIC algorithm (2) was performed only using $\hat{\mathbf{R}}_b$, and the results are shown in Fig. 10. Here, a source that was

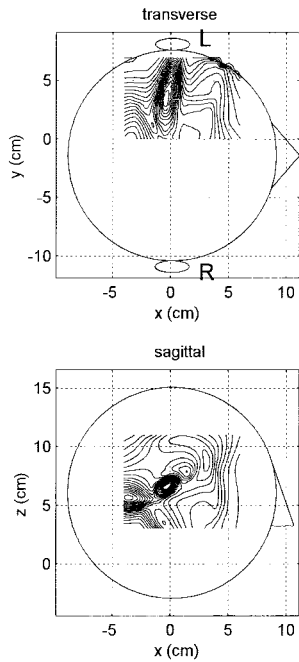


Fig. 9. The results of applying the nonprewhitening MUSIC algorithm to the averaged field data shown in Fig. 8. The covariance matrix $\hat{\mathbf{R}}_b$ was calculated using (5) with the time window between 30 and 130 ms.

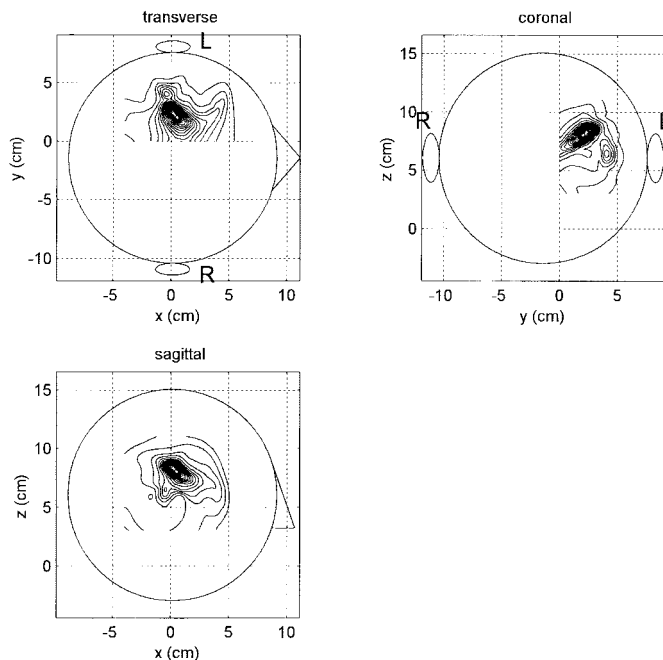


Fig. 10. The results of applying the nonprewhitening MUSIC algorithm to nonaveraged data having the artificial time jitter. The covariance matrix $\hat{\mathbf{R}}_b$ was calculated using (8) with the time window between 30 and 130 ms.

probably caused by the spontaneous background activity was detected, instead of the N1m source in the auditory cortex area. Next, we applied the prewhitening MUSIC algorithm using both covariance matrices $\hat{\mathbf{R}}_b$ and $\hat{\mathbf{R}}_n$. The results are shown in Fig. 11. Here, the N1m source was clearly detected. The comparison between Figs. 9 and 11 demonstrates the effectiveness of the proposed analysis for detecting a source with a time jitter at its activation onset. The comparison

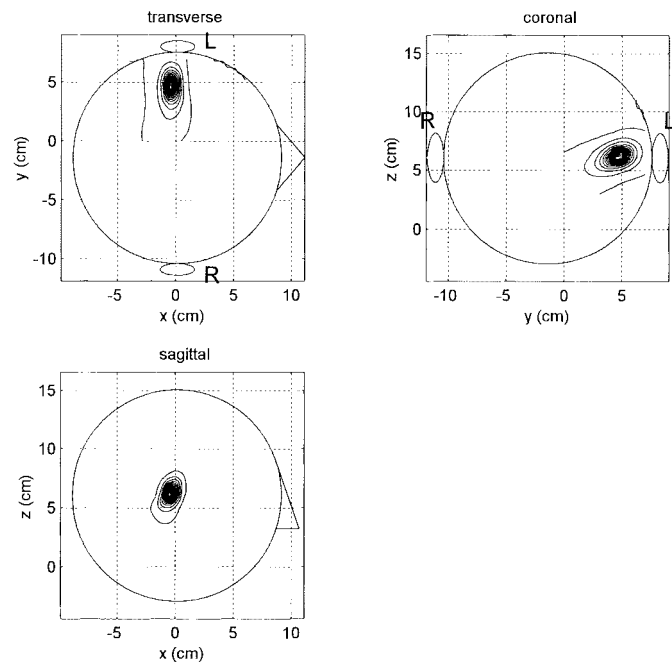


Fig. 11. The results of applying the prewhitening MUSIC algorithm to nonaveraged data having the artificial time jitter. The same covariance matrix $\hat{\mathbf{R}}_b$ as used to obtain the results in Fig. 10 was used. The noise covariance matrix $\hat{\mathbf{R}}_n$ was calculated with the time window between -240 and 0 ms.

between Figs. 10 and 11 again demonstrates the necessity and effectiveness of the prewhitening technique used here.

IV. CONCLUSION

A spatio-temporal analysis is proposed in which the measurement-covariance matrix is calculated by using the nonaveraged multiple-epoch evoked data. The proposed analysis has two advantages. First, a very narrow time window can be used. Second, the analysis can provide accurate localization of a source whose activation onset has a time jitter in each epoch. Experiments using measured auditory evoked data clearly showed that these advantages were obtained by using the proposed covariance matrix.

ACKNOWLEDGMENT

The authors wish to thank S. Honma and Dr. T. Roberts for their help in performing auditory MEG measurements.

REFERENCES

- [1] M. Scherg and D. von Cramon, "Two bilateral sources of the late AEP as identified by a spatio-temporal dipole model," *Electroencephalography. Clin. Neurophysiol.*, vol. 62, pp. 32–44, 1985.
- [2] ———, "A new interpretation of the generators of BAEP waves I–V: Results of a spatio-temporal dipole model," *Electroencephalography. Clin. Neurophysiol.*, vol. 62, pp. 290–299, 1985.
- [3] M. Hämäläinen, R. Hari, R. J. Ilmoniemi, J. Knuutila, and O. V. Lounasmaa, "Magnetoencephalography—theory, instrumentation, and applications to noninvasive studies of the working human brain," *Rev. Mod. Phys.*, vol. 65, pp. 413–497, 1993.
- [4] K. Sekihara, S. Miyauchi, and H. Koizumi, "Covariance incorporated MEG-MUSIC algorithm and its application to detect SI and SII when large background brain activity exists," *Neuro. Image*, vol. 3, no. 3, p. 92, June 1996.
- [5] K. Sekihara, D. Poeppel, A. Marantz, H. Koizumi, and Y. Miyashita, "Noise covariance incorporated MEG-MUSIC algorithm: A method for

multiple-dipole estimation tolerant of the influence of background brain activity," *IEEE Trans. Biomed. Eng.*, vol. 44, pp. 839–847, 1997.

- [6] A. Achim, François Richer, and J.-M. Saint-Hilaire, "Methodological considerations for the evaluation of spatio-temporal source models," *Electroencephalogra. Clin. Neurophysiol.*, vol. 79, pp. 227–240, 1991.
- [7] J. Sarvas, "Basic mathematical and electromagnetic concepts of the biomagnetic inverse problem," *Phys. Med. Biol.*, vol. 32, pp. 11–22, 1987.
- [8] J. C. Mosher, P. S. Lewis, and R. M. Leahy, "Multiple dipole modeling and localization from spatio-temporal MEG data," *IEEE Trans. Biomed. Eng.*, vol. 39, pp. 541–557, 1992.



Kensuke Sekihara (M'88) received the M.S. degree in 1976 and the Ph.D. degree in 1987, both from the Tokyo Institute of Technology, Tokyo, Japan.

Since 1976, he has worked with Central Research Laboratory, Hitachi, Ltd., Tokyo, Japan. He was a Visiting Research Scientist at Stanford University, Stanford, CA, from 1985 to 1986, and at Basic Development, Siemens Medical Engineering, Erlangen, Germany, from 1991 to 1992. He is currently working with the "Mind Articulation" research project sponsored by the Massachusetts

Institute of Technology and the Japan Science and Technology Corporation. His research interests include biomagnetic inverse problems and statistical estimation theory, especially its application to noninvasive measurements of brain functions.

Dr. Sekihara is a member of the IEEE Medicine and Biology Society, the IEEE Signal Processing Society, and the International Society of Magnetic Resonance in Medicine.

David Poeppel received the B.S. and Ph.D. degrees in cognitive neuroscience at Massachusetts Institute of Technology (MIT), Cambridge, in 1990 and 1995, respectively.

He is currently an Adjunct Assistant Professor in the Department of Radiology, University of California, San Francisco, and Assistant Professor in the Departments of Linguistics and Zoology at the University of Maryland at College Park. His research uses the functional neuroimaging methods magnetoencephalography (MEG) and functional magnetic resonance imaging (fMRI) to investigate the neural basis of speech and language processing.



Alec Marantz received the B.A. degree in psycholinguistics from Oberlin College, Oberlin, OH, in 1978 and the Ph.D. degree in linguistics from the Massachusetts Institute of Technology (MIT), Cambridge, MA, in 1981.

He joined the faculty at MIT in 1990, where he is currently a Professor of Linguistics in the Department of Linguistics and Philosophy. His research interests include the syntax and morphology of natural languages, linguistic universals, and the neurobiology of language. He is currently involved

in revising morphological theory within linguistics and in exploring MEG techniques to uncover how the brain processes language.



Hideaki Koizumi was born in Tokyo, Japan, in 1946. He graduated from the Department of Pure and Applied Sciences, the University of Tokyo, Tokyo, Japan, in 1971. He received the doctoral degree in physics from the University of Tokyo in 1976 for his thesis "Creating Polarized Zeeman-Effect Atomic Absorption Spectrometry."

He joined Hitachi, Ltd. Tokyo, Japan, in 1976. He was a member of the Visiting Faculty at the Lawrence Berkeley Laboratory, University of California, Livermore, CA, from 1978 to 1979. Upon

returning to Japan, he led MRI development projects. He now leads projects on environmental measurement and analysis, and noninvasive higher-order brain function analysis. He is a Chief Research Scientist at the Central Research Laboratory, Hitachi, Ltd. and Professor of the Research Institute for Electronic Science, Hokkaido University, Sapporo, Japan.

Dr. Koizumi received many awards such as the Ohkochi Memorial Prize, the Prize of Science and Technology Minister, and the IR-100. He is a member of the Board of Directors of the Chemical Society of Japan.



Yasushi Miyashita received the Ph.D. degree in physiology from the University of Tokyo, Tokyo, Japan, in 1979.

He is currently a Professor and Chairman of the Physiology Department, the University of Tokyo School of Medicine, Tokyo, Japan. His research interests include neural basis of cognition in primates, functional imaging, and image processing with MRI, MEG, and optical devices.